Channel Measurements and Path loss Modeling for Indoor THz Communication

Naveed A. Abbasi, Arjun Hariharan, Arun Moni Nair, Andreas F. Molisch
Wireless Devices and Systems Group (WiDeS)
Viterbi School of Engineering
University of Southern California
Email: {nabbasi, arjunhar, moninair, molisch}@usc.edu

***Abstract*—To explore the eventual deployment of communication systems in Terahertz (THz) band (0.1-10 THz) frequencies, extensive channel measurement campaigns are essential. In this regard, we conducted an indoor line-of-sight (LoS) measurement campaign up to 5.5 m on a THz channel sounding system that covers 140-220 GHz. We use a frequency-domain channel sounder that is based on a vector network analyzer (VNA) and frequency extenders for these measurements. Using the log-distance path loss model, we estimate the values of path loss exponent and the fading distribution standard deviations. The power delay profile analysis of our measurements shows that there are negligible multipaths in the LoS channels for the current scenario. Our results provide a platform for future exploration of THz band communication in the 140-220 GHz frequency range.**

***Index Terms*—Terahertz (THz) communication, indoor scenario, frequency-domain channel sounding, line-of-sight channels.**

I. Introduction

The demands for higher data rates to cater for applications such as high-resolution videos and 3D experience environments are increasing constantly. In order for the technology to satisfy consumer needs, next-generation wireless networks need to realize data rates reaching terabits per second (Tbps) while also supporting higher connection density [1]–[3]. The 60 GHz spectrum is expected to increase data rates to 6 Gbits/s [4], however, the available spectrum around this frequency is limited to 9 GHz. Consequently, it may not fully satisfy the bandwidth requirements for long. To support high throughputs on the order of Tbps, enormous bandwidth is required along with higher area spectral efficiency. Hence, researchers around the world are exploring the Terahertz (THz) Band (0.1 - 10 THz) [5]–[10]: very large swaths of spectrum are either available now, or are expected to become available in the future.

At the same time the directional nature of THz propagation, combined with the potential of building antenna arrays with a large number of elements ($>$ 1000) that can be fit into a reasonable form factor are quite attractive [11], [12]. Although THz communication presents an interesting opportunity, a number of challenges are faced by potential communication schemes in this band. Higher frequencies, being highly directional, are more easily blocked by any obstacles on their path. Moreover, atmospheric characteristics also play a major part in communication links operating above 100 GHz, since molecular absorption may lead to high signal losses. We should also note that the ultimate application of a communication scheme is highly dependent on the scenario for its use as well. For instance, large coverage areas, high speed and fast moving networks each pose their own set of challenges. To properly assess the potential and limitations of THz communications, we first need knowledge of propagation channel characteristics, which have to be obtained from measurements. In this regard, recent interest by Federal Communication Commission (FCC) is noticeable where sub-bands in the THz band between 140-220 GHz were earmarked for experimental licenses to encourage research [13].

Up to now, most of the interest for THz communications has concentrated on short range indoor scenarios, such as infostations in the 300 GHz band [14]–[17]. In this study, we present THz band channel measurements in the 140-220 GHz for a line-of-sight (LoS) indoor office scenario. We perform three independent measurements, each with 11 different measurement point between 0.5 and 5.5 m to characterize these LoS channels. Pathloss exponent and the standard deviation of the fading distribution for the log-distance path loss model are estimated for three sub-bands in the 140-220 GHz range, namely, the 140-150 GHz band, 180-190 GHz band and the 210-220 GHz band. Furthermore, power delay profile (PDP) analysis for various measurements show that this particular indoor THz network does not have significant multipath components in LoS scenarios.

The rest of this paper is organized as follows. The measurement equipment and site is described in Section II. Section III highlights the major results for our measurement campaign. Finally, the manuscript is concluded in Section IV.

II. Measurement Equipment and Site

Experimentation in the THz band is rather difficult due to extremely small wavelengths (1 - 0.1 mm) and the strong signal attenuation by components such as cables that is generally unproblematic at lower frequencies. The measurements presented in the current manuscript were conducted with a custom configured frequency-domain channel sounder. In this section, we describe the testbed used for the experimentation and provide details of the measurement site.

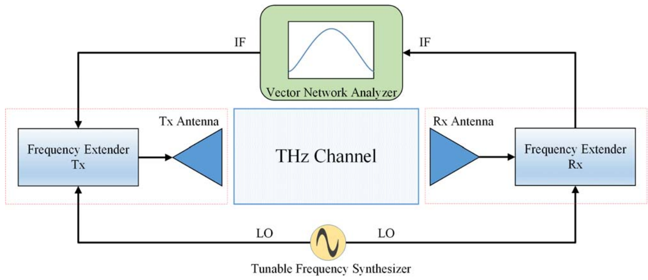

Fig. 1: VNA-based THZ measurement setup.

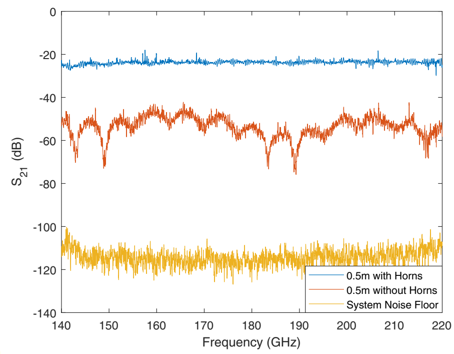

Fig. 2: Comparison of the setup with and without directional horns.

A. Testbed Description

Measurement of wideband channel characteristics, which are the focus of our interest, can be conducted either by time-domain [18] or frequency-domain [15] setups. As discussed earlier, our current work is based on a frequency-domain setup. Such setups are generally known to provide excellent robustness and often act as ground truths for time-domain setups.

A diagram of our THz equipment is shown in Fig. 1. A VNA produces Intermediate Frequency (IF) signals that are then mixed by special frequency extenders with signals from a Local Oscillator (LO) that is operating in the THz range. This THz LO signal is generated by a frequency synthesizer and it is then multiplied up into the THz range in the frequency extenders. In case the VNA has more than 2 ports, it can also produce LO signals required by the setup in Fig. 1, obviating the need for a separate frequency synthesizer. In our work, we use a 4-port VNA by Keysight Technologies (N5247A) that operates in the 0.01 - 67 GHz range to generate all the LO and the IF signals.

For the frequency extension, we use an extender set produced by Virginia Diodes Inc (VDI) that operates in the range of 140 - 220 GHz range. In order to reach the THz band, the LO signal (11.67 GHz to 18.33 GHz) is multiplied by a factor of 12. The dynamic range of these extenders is on the order of 140 dB for a special high sensitivity mode, however, for the current short distance indoor configuration we chose the standard sensitivity mode that has a reduced dynamic range of around 120 dB. The THz sounding signal (mixing product of IF and multiplied LO) is radiated from the transmitter (Tx) via a directional horn antenna. The reception and downconversion at the receiver (Rx) is completely analogous. It should be noted here that the frequency extenders can have a number of different configurations and though a detailed discussion on the merits of these is beyond the scope of this paper, we make a note that our setup uses the through-reflect configuration since we are mostly interested in transmission characteristics of the channel.

The setup was calibrated before the measurement campaign to separate the characteristics of the equipment from the channel. The calibration was performed with a VDI calibration kit and horn antennas (also from VDI) were added after the calibration. The calibration process reduces the effective length of the channel by 0.15 m since it has to compensate for two waveguides (one at Tx and the other at Rx) that connect the horn antennas with the extenders themselves. Each horn antennas is rated for a gain of 21 dBi with a beam width of 13°. Fig. 2 shows a comparison of the setup with and without horn antennas for a channel length of 0.5 m. We can see that the horn antennas offer a significant improvement in the transmission power and, therefore, we use horns antennas for all the other results reported in this manuscript.

B. Site Description

As discussed earlier, scenarios are themselves a very important factor in any channel sounding campaign. For the current measurement, we investigate an indoor scenario. The WiDeS lab was used for this campaign which is similar to a typical office environment with desks and chairs. During the course of the measurement, the equipment area was closed to maintain a static environment. We used laser crosshairs and pointers for the alignment of the frequency extenders after the hardware deployment to ensure that the extenders are maintained at the same height from the ground and are looking directly at each other. An overview of the site is shown in Fig. 3 where a Tx and corresponding Rx measurement positions are shown. As

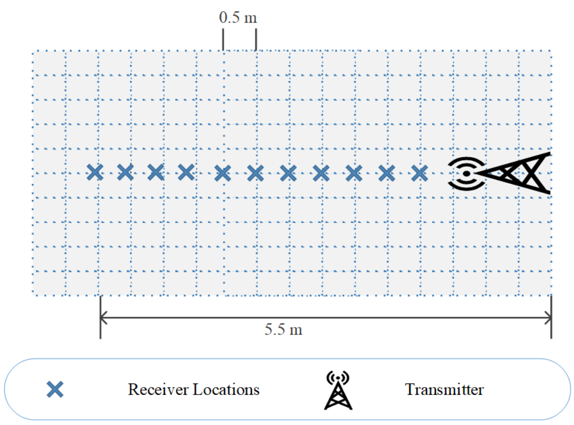

Fig. 3: Site map for measurement campaign.

TABLE I: Setup parameters.

Parameter	Symbol	Value
Measurement points	N	5000
Averaging factor	Avg	10
Start frequency	f_{start}	140 GHz
Stop frequency	f_{stop}	220 GHz
Bandwidth	BW	80 GHz
IF Bandwidth	IF_{BW}	500 Hz
THz IF	f_{THzIF}	279 MHz

described earlier, three different sets of measurements were performed where the Tx was moved after each measurement and the Rx was moved correspondingly to various distances between 0.5 m and 5.5 m.

III. Measurement Results

In this section, we present some of our key measurement methodologies and the associated results.

A. Measurement Parameters

A summary of key measurement parameters, their acronyms and nominal values is given in Table I. The selection of 5000 points over 80 GHz of bandwidth gives us a frequency resolution 16 MHz which translates to 0.0625 μs excess delay or 18.75 m excess distance that an existing multipath may travel in order for the system to detect it. Under the current indoor office scenario, we believe that this provides sufficient information regarding the multipath environment in the channel.

B. LoS Measurement

Using the parameters discussed in Table I, we performed a total of 33 LoS channel measurements for covering various distances and Tx/Rx placements. The LoS path loss measurements for one particular case are shown in Fig. 4. The trend of this results seems to suggest that the path loss is increasing by a log-distance mechanism. Measurement-to-measurement variation in path loss between three channels of 1 m length are shown in Fig. 5. Results show that although variations in different measurements over the same distance are present, the average value of path loss over the band will be pretty similar for all of them.

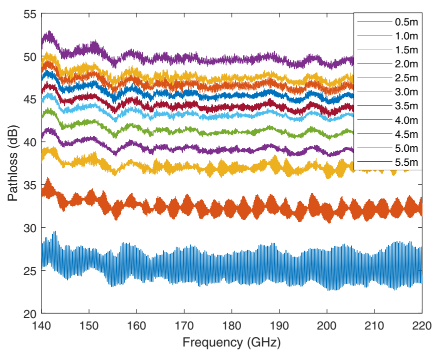

Fig. 4: LoS Measurements for various distances.

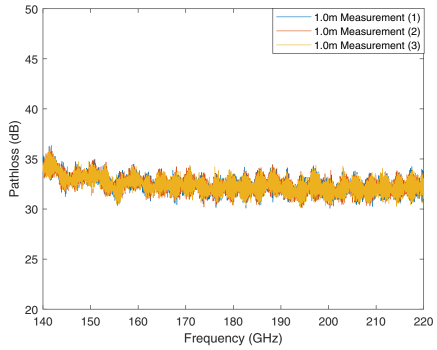

Fig. 5: Measurement-to-measurement variation for one particular distance.

TABLE II: Estimated parameters.

Band	γ	σ
140-150 GHz	2.117	0.5712
180-190 GHz	2.249	0.7229
210-220 GHz	2.229	0.7126

C. Log-distance Path loss Model

For an observed channel, path loss over a particular distance can be modeled by the log-distance path loss model as [19]

$$\overline{PL}(d) = PL(d_0) + 10\,\gamma\, log(\frac{d}{d_0}) + X_\sigma, \qquad (1)$$

where, $\overline{PL}(d)$ is the average path loss in decibels at the distance d, γ is the path loss exponent which indicates the rate at which the path loss increases with d, $PL(d_0)$ is the path loss at reference distance d_0 and X_σ is a zero-mean Gaussian distributed random variable (in dB) with standard deviation σ (also in dB). Assuming that the model holds for the current scenario, we used MATLAB's *'cftool'* to estimate the γ and σ, and considered d_0 = 0.35 m (0.5 m with 0.15 m compensated for the waveguides). These results are presented in Table II. The measurements and the fitted curves are shown in Fig. 6 for three frequency sub-bands in our overall range. These results are further compared against the free-space path loss (FSPL) model given by,

$$FPSL(d) = 20log(\frac{4\pi df}{c}) - G_{Tx} - G_{Rx}, \qquad (2)$$

where, G_{Tx} and G_{Rx} are the transmit and the receive antenna gains (21 dB in the current case) and f is the center frequency of the band in question. The results in Fig. 6 show that the log-distance path loss model fits well with the measurement points. Moreover, we see that FPSL can be used a rough estimate particularly at the lower end of the frequency band.

D. Power Delay Analysis

The PDPs for various distances in a set of measurements is shown in Fig. 7 after a compensation of 0.15 m for the waveguides. It can be seen that for all the cases shown here, we can identify the major transmitted components easily in

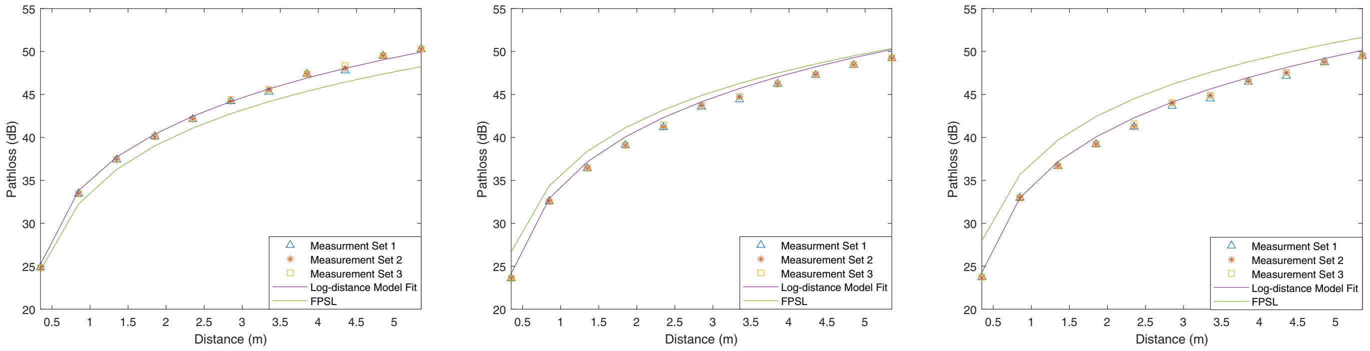

(a) 140-150 GHz band. (b) 180-190 GHz band. (c) 210-215 GHz band.

Fig. 6: Measurements and path loss models for various frequency bands.

the delay domain. Moreover, except for the 0.5 m case, there are no major multipath components present in any other LoS measurement. This results alludes to the high directionality of THz channels and the small beam width of the Tx and Rx horn antennas. Further detailed knowledge about the multipath environment can be achieved by means of double directional channel measurements that we plan to perform in future.

IV. Conclusion

In this paper, we present a set of indoor measurements performed in an office environment for the THz frequency band between 140-220 GHz. The range of measurement distances varies from 0.5 to 5.5 m as would be expected in an office environment. Our results show that the log-distance path loss model can be applied in the current scenario and the values of path loss exponents for various sub-bands in the overall range are around 2.1-2.2. Moreover, we observe that the signal and its multipaths are separable in the delay domain where we see negligible amount of multipaths for the LoS channels. In our future work, we plan to investigate further indoor and outdoor scenarios, as well as multiple-input multiple-output (MIMO) channels.

V. Acknowledgment

This work was supported by the Semiconductor Research Corporation (SRC) under the ComSenTer program. We thank Dr. Todd Younkin (SRC), Prof. Mark Rodwell (UCSB) and the WiDeS team for helpful discussions.

References

[1] K.-C. Huang and Z. Wang, "Terahertz Terabit Wireless Communication," *Microwave Magazine, IEEE*, vol. 12, no. 4, pp. 108–116, June 2011.

[2] V. Chandrasekhar, J. G. Andrews, and A. Gatherer, "Femtocell networks: a survey," *IEEE Communications Magazine*, vol. 46, no. 9, pp. 59–67, September 2008.

[3] M. Shafi, A. F. Molisch, P. J. Smith, T. Haustein, P. Zhu, P. D. Silva, F. Tufvesson, A. Benjebbour, and G. Wunder, "5G: A Tutorial Overview of Standards, Trials, Challenges, Deployment and Practice," *IEEE Journal on Selected Areas in Communications*, 2017.

[4] IEEE, "Part 15.3: Wireless Medium Access Control and Physical Layer Specifications for High Rate Wireless Personal Area Networks," 2009.

[5] N. Khalid, N. A. Abbasi, and O. B. Akan, "Capacity and coverage analysis for fd-mimo based thz band 5g indoor internet of things," in *Personal, Indoor, and Mobile Radio Communications (PIMRC), 2017 IEEE 28th Annual International Symposium on*. IEEE, 2017, pp. 1–7.

[6] ——, "Statistical characterization and analysis of low-thz communication channel for 5g internet of things," *Nano Communication Networks*, p. 100258, 2019.

[7] A. Hirata and M. Yaita, "Ultrafast Terahertz Wireless Communications Technologies," *IEEE Transactions on Terahertz Science and Technology*, vol. 5, no. 6, pp. 1128–1132, Nov 2015.

[8] I. F. Akyildiz, J. M. Jornet, and C. Han, "TeraNets: ultra-broadband communication networks in the terahertz band," *IEEE Wireless Communications*, vol. 21, no. 4, pp. 130–135, August 2014.

[9] H. J. Song and T. Nagatsuma, "Present and Future of Terahertz Communications," *IEEE Transactions on Terahertz Science and Technology*, vol. 1, no. 1, pp. 256–263, Sept 2011.

[10] T. Kürner and S. Priebe, "Towards THz Communications - Status in Research, Standardization and Regulation," *Journal of Infrared, Millimeter, and Terahertz Waves*, vol. 35, no. 1, pp. 53–62, 2014.

[11] Y. Kim, H. Ji, J. Lee, Y.-H. Nam, B. L. Ng, I. Tzanidis, Y. Li, and J. Zhang, "Full dimension mimo (fd-mimo): The next evolution of mimo in lte systems," *IEEE Wireless Communications*, vol. 21, no. 2, pp. 26–33, 2014.

[12] N. Khalid, N. A. Abbasi, and O. B. Akan, "300 ghz broadband transceiver design for low-thz band wireless communications in indoor internet of things," in *Internet of Things (iThings) and IEEE Green Computing and Communications (GreenCom) and IEEE Cyber, Physical and Social Computing (CPSCom) and IEEE Smart Data (SmartData), 2017 IEEE International Conference on*. IEEE, 2017, pp. 770–775.

[13] FCC, "Fcc takes steps to open spectrum horizons for new services and technologies," http://https://docs.fcc.gov/public/attachments/DOC-356588A1.pdf, 2019.

[14] M. Y.-W. Chia, B. Luo, and C. K. Ang, "Extremely wideband multipath propagation channel from 285 to 325 ghz for a typical desk-top environment," in *Infrared Millimeter and Terahertz Waves (IRMMW-THz), 2010 35th International Conference on*. IEEE, 2010, pp. 1–1.

[15] S. Priebe, C. Jastrow, M. Jacob, T. Kleine-Ostmann, T. Schrader, and T. Kürner, "Channel and propagation measurements at 300 GHz," *Antennas and Propagation, IEEE Transactions on*, vol. 59, no. 5, pp. 1688–1698, 2011.

[16] S. Kim and A. G. Zajić, "Statistical characterization of 300-ghz propagation on a desktop," *IEEE Transactions on Vehicular Technology*, vol. 64, no. 8, pp. 3330–3338, 2015.

[17] S. Kim and A. Zajić, "Characterization of 300-ghz wireless channel on a computer motherboard," *IEEE Transactions on Antennas and Propagation*, vol. 64, no. 12, pp. 5411–5423, 2016.

[18] Y. Xing and T. S. Rappaport, "Propagation measurement system and approach at 140 ghz-moving to 6g and above 100 ghz," in *2018 IEEE Global Communications Conference (GLOBECOM)*. IEEE, 2018, pp. 1–6.

[19] T. S. Rappaport *et al.*, *Wireless communications: principles and practice*. Prentice Hall PTR New Jersey, 1996, vol. 2.

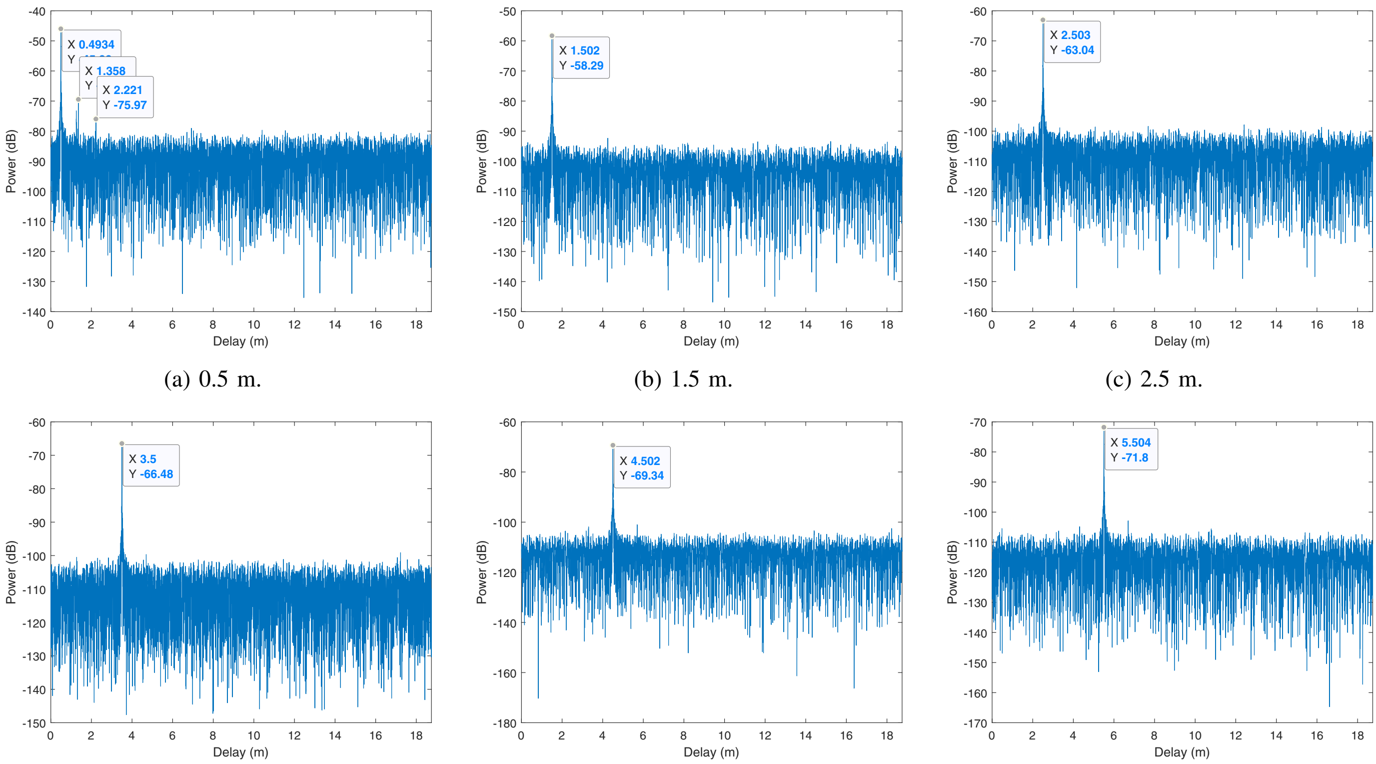

(a) 0.5 m. (b) 1.5 m. (c) 2.5 m.

(d) 3.5 m. (e) 4.5 m. (f) 5.5 m.

Fig. 7: PDPs for measurements of different distances.